LA-UR-01-6142
Approved for public release;
distribution is unlimited.

Title: **Refractory Metal Welding Using a 3.3 kW Diode Pumped Nd:YAG Laser**

Author(s): J.O. Milewski, R.W. Carpenter II,
R. Nemec, A. Kelly, M.S. Piltch

Submitted to: Proceeding of the International Conference on Joining of Advanced and Specialty Materials

ASM International
Indianapolis, IN
November 6, 2001

Refractory Metal Welding Using a 3.3 kW Diode Pumped Nd:YAG Laser

J.O. Milewski, R.W. Carpenter, R. Nemec, A. Kelly, M.S. Piltch
Los Alamos National Laboratory
Metallurgy Group, Materials Science and Technology Division

Abstract

Recent developments in multi-kilowatt continuous wave lasers allow fiber optic delivery to high-purity controlled atmosphere chambers and challenge electron beam welding with improvements in cost, complexity, beam quality and flexibility. Questions remain with respect to the performance of these lasers for refractory alloy welding regarding damaging back reflections, laser-plume interactions, and sufficiency of beam intensity and coupled energy. System performance for the welding of various refractory metal alloys and comparisons to electron beam welds will be presented.

Introduction

Refractory metals are high melting point elements from Group VA, VIA, include rhenium from Group VIIA, and range in atomic number from 23 (Va) to 75 (Re). They generally include the metals Va, Nb, Mo, Ta, W, Re and their alloys. They posses a body centered cubic crystallographic structure except rhenium which is hexagonal in structure. These materials are often alloyed with each other and Group IVA reactive metals in small amounts to provide a wide range of unique properties. They are less abundant than common engineering metals, generally more costly, and therefore limited in the range of commercially available forms. In addition, processing of many of these alloys can be difficult as a result of their reactivity and mechanical properties

Figure 1 provides a listing of the properties of the pure forms of these materials. As a result of these unique properties and associated costs, selection of these materials is often reserved for specialty or advanced applications.

Examples of specialty applications include the high temperature use of refractory metals in space power systems and cryogenic applications of ultra pure niobium in superconducting particle accelerator applications. The use of refractory metals in space reactor and associated energy conversion system technology is primarily driven by its high temperature structural properties, compatibility with fuel and other materials within the reactor environment, and ability for alkali liquid metal containment. Physical and mechanical property considerations include strength at temperature, high temperature creep properties and high thermal conductivity to transport heat out of the reactor core into heat transport and energy conversion systems [1-5].

	Va	Nb	Mo	Ta	W	Re
T_m K	2175	2740	2890	3287	3680	3453
T_v K	3682	5017	4912	5731	5828	5869
Density @ 300 K g/cm3	5.8	8.6	10.2	16.6	19.3	21.0
Thermal conductivity W cm^{-1} K^{-1}	0.31	0.54	1.38	0.58	1.74	0.48
Electrical Conductivity 10^6 O^{-1} cm^{-1}	0.049	0.069	0.187	0.076	0.19	0.05

Figure 1. Properties of pure refractory metals.

Under cryogenic operating conditions, niobium is used in the fabrication of radio frequency (RF) accelerator cavities due to its superconducting properties, adequate mechanical strength at cryogenic temperatures and relative fabricability [6].

Refractory metal joining technology had it origins in the 1950's and 1960's where significant alloy and process development was performed to evaluate their properties and the effects of processing refractory metals with its short and long-term performance. Strength, creep and corrosion performance at high temperatures can be greatly affected by contamination by impurities during weld processing. These impurities include low melting point elements which segregate to grain boundaries during solidification which increase the propensity for hot cracking, decreased strength and corrosion resistance. Contamination with oxygen, nitrogen and hydrogen at elevated temperatures lead to the interstitial penetration of these elements into the structure of the weld region and can significantly reduce

the performance of the heat affected and fusion regions of the weld. A recent general reference is provided by Olson Et al. [7].

Early development of joining processes for refractory metal welding included the development of acceptable processing techniques to limit contamination during forming, machining, cleaning and handling. For fusion welding, this includes compatible materials for fixturing and heat sinking as well as acceptable levels of purity for inert atmosphere weld chambers. The low energy density, high heat input, and relatively slow solidification rates of arc welding, promotes the formation of large grain growth in the fusion zone and heat affected zones. These large grains segregated impurities at the fewer grain boundaries that localizes weakness in the weld microstructure and generally decrease desirable properties within the weld region. An example of a large detrimental grain growth in a GTA weld made in Nb1Zr is shown in Figure 2.

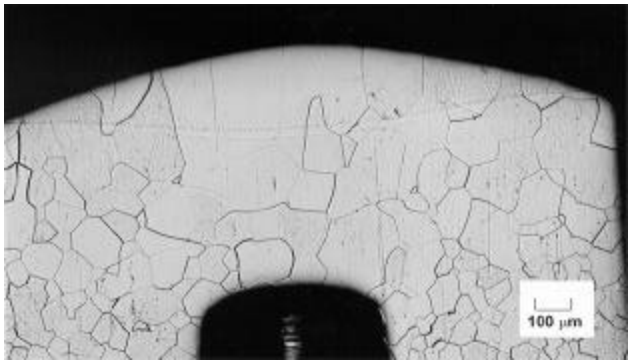

Figure 2. Large grain growth in a Nb1Zr Gas Tungsten Arc weld.

Electron Beam Welding

The development of electron beam (EB) welding has allowed high energy density welding at higher speeds resulting in deep narrow welds and reduced heat input. This allowed significantly increased cooling rates, improved microstructures (reduced grain growth) and ultimately improved short and long term performance. Additional advantages of EB welding include high precision beam generation, accurate beam delivery and high purity welding in a vacuum chamber. Disadvantages include high equipment costs, system complexity (high voltage, vacuum, electron beam generation/optics), vacuum chamber constraints, required maintenance levels and a greater potential for mixed waste streams when applied to nuclear applications.

Laser Beam Welding

Laser beam weld processing has seen significant development in the past 20 years. Application of mutli-kilowatt CO_2 laser cutting, welding and pulsed welding, using solid state lasers, has seen widespread application in industry. Development of continuous wave, multi-kilowatt Nd:YAG lasers, capable of fiber optical delivery, has within the past five years, extended the capabilities of these systems to produce welds in controlled environments previously performed by the EB weld process. The 1.06 µm wavelength of Nd:YAG lasers allows easy transport laser energy through windows and optical fibers thus facilitating the introduction of high power laser energy for welding into controlled atmosphere glove box enclosures. Los Alamos National Laboratory has for many years been involved in technology development requiring the fabrication and joining of refractory metal components. These needs have historically been met using EB welding and brazing processes. The recent installation of a 3.3 kW, diode pumped Nd:YAG laser, combined with renewed interest in refractory metal joining for nuclear applications, provide the motivation for evaluation of this new capability for the joining of refractory metals. The study will focus on preliminary results of laser weld penetration and morphology for various refractory metals, analysis of system performance and critical comparison of laser verses EB weld processing.

Diode Pumped, Continuous Wave, Nd:YAG : Principals of Operation

A diagram of a diode pumped laser cavity is given in Figure 3. Replacement of conventional flash lamps with diode bars allows pumping the laser rod with a narrow frequency band of light verses the wide band pumping of conventional flash lamps. These specific frequencies are more highly absorptive to the crystal media, producing higher efficiency, reduced heating, thermal lensing of the rod, unwanted distortions, and reduced beam quality. This allows for smaller less divergent laser beams and delivery using smaller optical fibers. Improved beam quality can reduce the size of output optics and produce larger F#s and small focal spot sizes. Deeper and narrower welds have been reported using this technology [8].

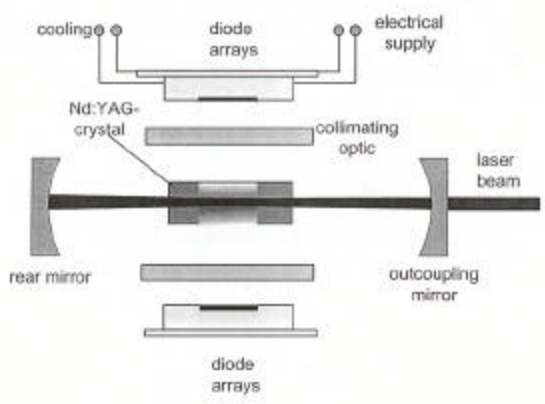

Figure 3. Diagram of a Diode Pumped Nd:YAG laser cavity. (Courtesy of Rofin-Sinar Inc.)

Experimental Conditions

Bead on plate welds were performed using diode pumped laser and electron beam welding equipment described in the table of Figure 4. A listing of the refractory alloys used and thickness are provided in the table of Figure 5. These materials and thickness represent a wide range of alloys and thicknesses typical to space power and nuclear applications. The materials were chemically cleaned using a nitric HF acid dip and rinsing in water They were clamped without backing or heat sinking. The

parameter settings used are provided in Figure 6. Individual weld passes were spaced 1 cm apart and allowed to cool ten minutes between adjacent weld passes. For the purpose of this preliminary study, they were welded in an inert glovebox purged with welding grade argon. Inert gas quality was indicated by welding upon Ti-6-4 alloy and observation of a light straw color prior to welding of the refractory metal samples. Weld top and bottom bead surfaces were examined prior to sectioning at a magnification of 10X.

Laser	Rofin-Sinar DY33
Type	CW Diode Pumped Nd:YAG
Power maximum	3.3 kW
Delivery fiber size	400 µm
Focal spot size	~500 µm
Focal length lens	120 mm
Purged glove box atmosphere	Welding grade argon
EB welder	Leybold-Heraeus
Type	High vacuum, high voltage
Power / voltage maximum	7.5 kW, 150 kV
Filament type	Tungsten ribbon
Focal spot size	~ 300 µm
Focal length	10-100 cm adjustable
Vacuum chamber atmosphere	< 10^{-4} torr

Figure 4. Equipment used in the study.

Material	Thickness mm	Joint Design
Nb1Zr	1.5	Bead on plate
ASTAR 811C	1.5	Bead on plate
Mo13Re	1.4	Bead on plate
Re	0.5	Bead on plate

Figure 5. Materials used in this study. The nominal composition of ASTAR 811C is (Ta-8W-1Re-1Hf-0.02C).

Laser power, kW	0.5, 1.0, 1.5, 2.0, 2.5, 3.3
Travel speed	115 cm/min, (45 ipm)
Focal condition	Sharp at surface
Laser beam tilt angle	10 degrees
EB power, kW	0.5, 1.0, 1.5
EB voltage, kV	100
Travel speed	115 cm/min, (45 ipm)
Focal condition	Sharp at surface

Figure 6. Parameters used in this study.

Welds were sectioned using water-cooled abrasive cutting, mounted and ground back to remove any potential cutting effect to the microstructure. They were polished using a 0.3 micron alumina slurry and etched using 56% lactic acid 33% HNO_3 and 11% HF to reveal weld morphology and microstructure.

Results and Observations

Visual examination of the electron beam welds showed melting at all power levels between 0.5 and 1.5 kW indicating the energy coupling and melting was easily achieved. Electron beam welds rapidly produced full penetration due to a smaller spot size and increased energy density of the beam. Increased undercutting of the root beads in all EB welds was observed at 1.5 kW.

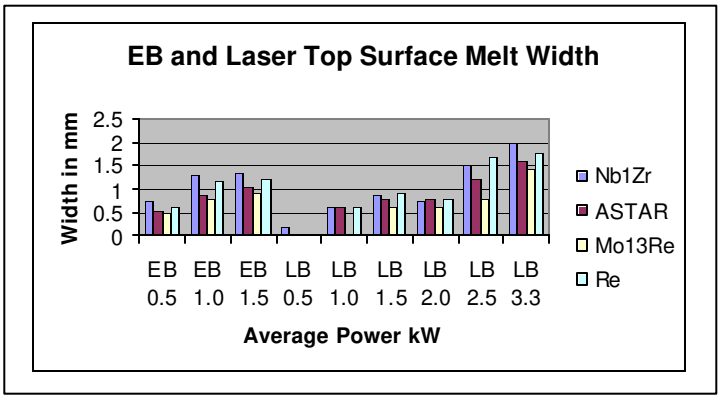

Figure 7. Top weld bead width for the power settings used.

Visual examination of the laser welds revealed a variation in the power required for the onset of conduction mode melting. This was expected by the variation in material properties and thickness. Top surfaces were smooth and bright in conduction mode melting. Increased surface roughness, spatter and vapor deposit adjacent to the fusion zone indicated increased vaporization and material expulsion from the weld pool at higher powers. Top bead weld width as a function of power is presented in the chart of Figure 7.

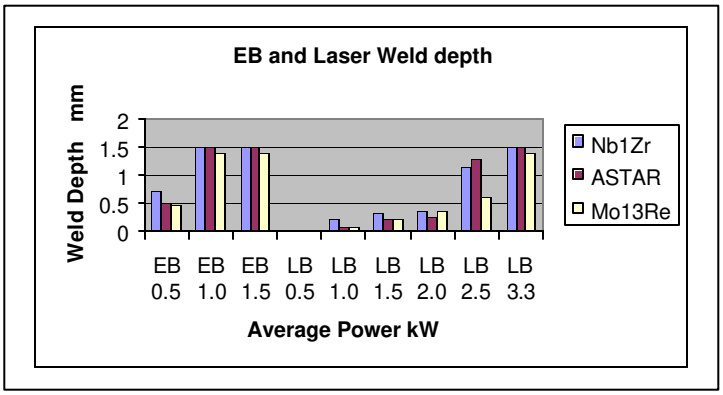

Figure 8. Weld depth as a function of power for three alloys.

The data shows the electron beam weld welds rapidly reach a steady width as full penetration was achieved over at 1 kW and above. Little to no melting was observed in the laser welds at 500 watts, aside from lowest melting Nb1Zr, due to the decreased energy coupling and energy intensity of the laser verses the electron beam. At 1 kW most laser welds reached the

melting threshold aside from Mo13Re due to its high melting point and high thermal conductivity.

Metallographic examination of transverse cross sections revealed the weld depths, as a function of average power as given in the chart of Figure 8. The electron beam welds rapidly achieved full penetration at 1.0 kW while the laser welds did not achieve melting until approximately 1 kW. The niobium and tantalum alloys transitioned into keyhole melting between 2.0 and 2.5 kW while the molybdenum alloy did not transition to a high aspect ratio keyhole weld until nearly 3 kW power was achieved. All laser welds, including Re, displayed full penetration at 3.3 kW.

Nb1Zr welds

Niobium 1% Zirconium welds displayed smooth top beads with observed top bead crowning at higher powers and in wider welds. Figures 9 and 10 show grain growth in the fusion region of both EB and laser welds to be of similar dimension.

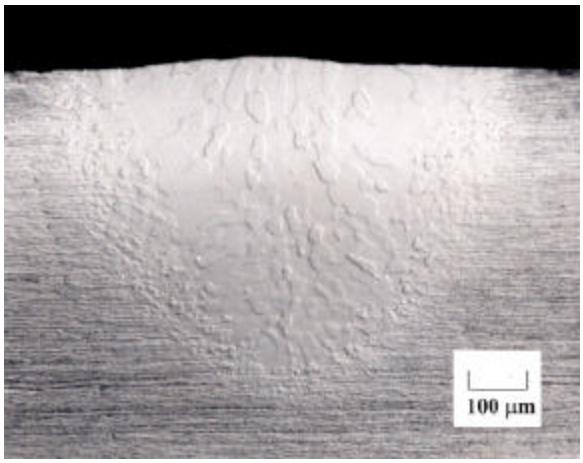

Figure 9. Grain growth in an EB weld at 500 watts in Nb1Zr.

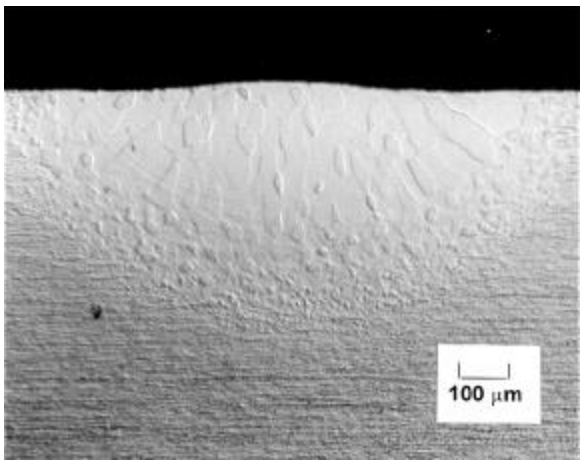

Figure 10. Laser weld at 1.5kW displaying similar grain size in the fusion region.

Higher power EB welds displayed increased top bead undercutting due to severe undercutting and material loss from the underside of the joint (Figure 11.). In practice, beam power or beam intensity would be reduced to alleviate this condition by reducing the beam amperage or defocusing the electron beam.

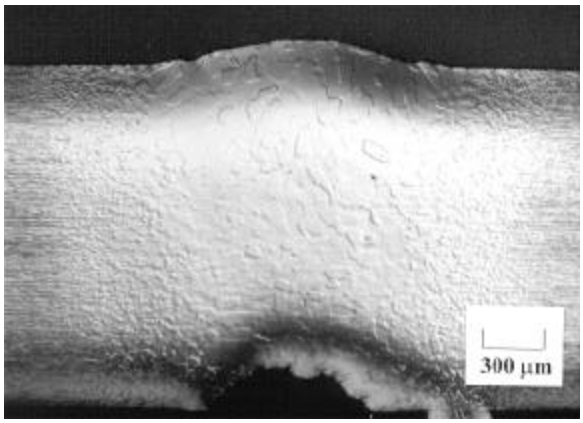

Figure 11 Undercutting observed one the root bead of an electron beam weld in Nb1Zr.

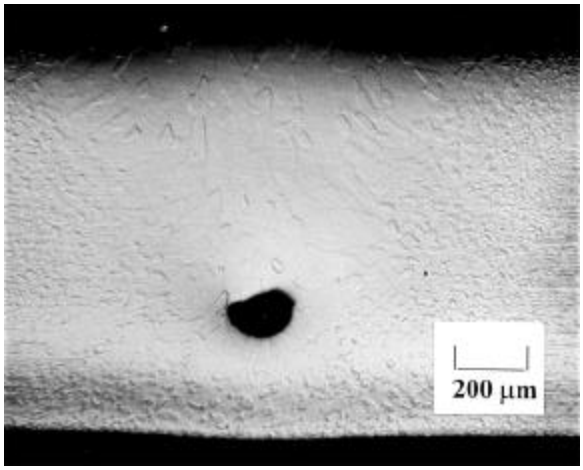

Figure 12. Entrapped void at the root of a laser weld in Nb1Zr.

Full penetration was observed only at 3.3 kW using this laser. Figure 12 shows an entrapped void at the root of this partial penetration keyhole weld

ASTAR 811C (Ta-8W-1Re-1Hf-0.02C).

Similar to the Nb1Zr welds, the EB welds displayed full penetration above 500 watts and a rough undercut root bead above 1 kW. The laser welds did not achieve full penetration until 3.3 kW was attained. The weld root under bead at 3.3 kW was smooth without any evidence of undercutting. Unlike the NB1Zr, no porosity or entrapped voids were observed in any of the ASTAR 811C welds. Figure 13 shows a high depth-to-width aspect ratio, full penetration. EB weld made at 1 kW. A very small heat affected zone is shown to have evolved. Despite the larger focal spot size, the laser weld shown in Figure 14 also display a high aspect ratio, although wider and displaying a wider heat affected zone adjacent to the fusion boundary.

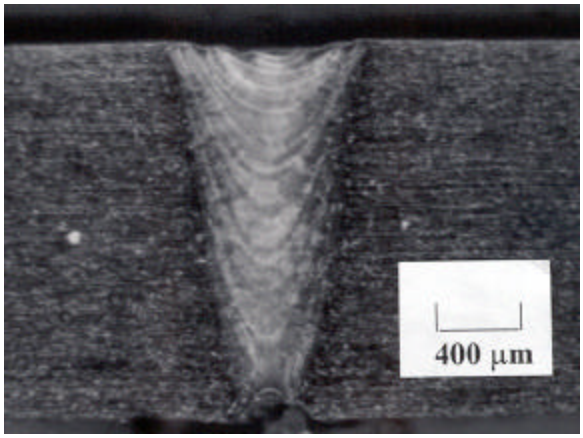

Figure 13. Electron Beam Weld in ASTAR 811C at 1.0 kW.

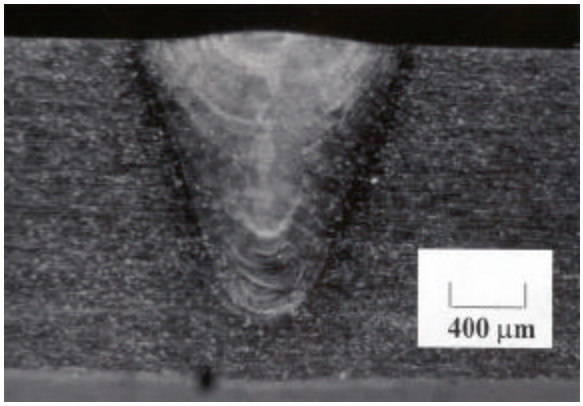

Figure 14. Laser Beam Weld in ASTAR 811C at 2.5 kW.

Molybdenum 13 wt. % Rhenium

As similar to the ASTAR 811C welds, the EB welds displayed full penetration above 500 watts and a rough undercut under bead above 1 kW. A wide recrystallized heat affected region is shown in the EB weld of Figure 15.

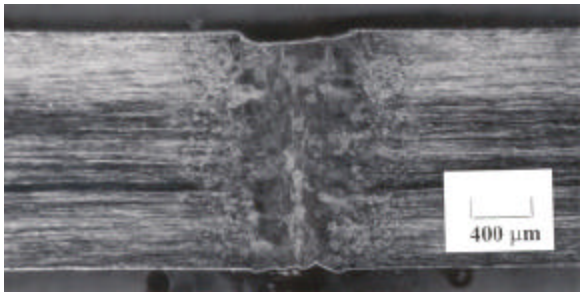

Figure 15. Grain Growth in an 1 kW EB weld in Mo13%Re.

The laser welds did not achieve coupling until 1.5 kW. Full penetration was not achieved until 3.3 kW was provided. The laser weld root under bead at 3.3 kW was smooth without any evidence of undercutting although significant grain growth in the fusion zone and heat affected zone is shown in Figure 16.

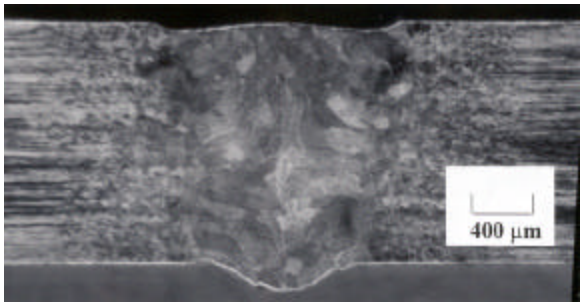

Figure 16. Heat affected zone in a Mo13%Re laser weld at 3.3 kW.

Rhenium

The rhenium metal was significantly thinner than the other refractory metals. As similar to the Nb1Zr welds, the EB welds displayed full penetration above 500 watts but unlike the other materials the under bead was always smooth. The laser welds did not achieve coupling until 1.0 kW. Full penetration was achieved at 2.5 kW. Difficulties in interpretation of the metallographic preparation prevented the reporting of accurate weld penetration data. The solidification patterns and grain growth, shown on the top bead surface of the macrograph of Figure 17, clearly show the intersection of the grain with the trailing solidification boundary, indicated by weld top bead rippling, occurs at an angle normal to the solidification front. Porosity was evident on the top bead surfaces, and within the fusion region as shown in the transverse section of an EB weld in Figure 18. No porosity was visible on the backside root bead surface. This is most likely due to the powder-processed origin of the base material. Lasers welds displayed a reduced level of porosity but large grain growth in the wider welds as shown in Figure 19, where the arrows above indicate the melt zone width.

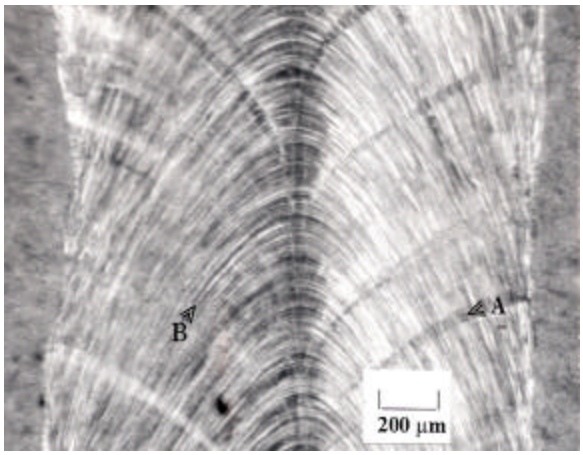

Figure 17. Laser welds in Rhenium display grain growth (A) as they maintain an orientation normal to the solidification boundary (B) as they solidify toward the weld centerline.

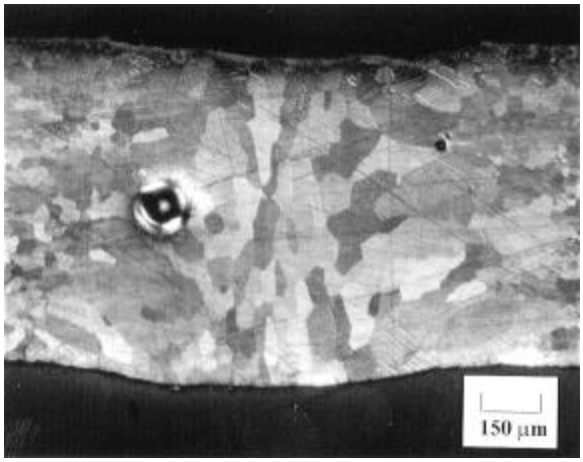

Figure 18. Electron Beam Weld in Re showing entrapment of coalesced gas porosity within the fusion zone.

Discussion

This preliminary work allows qualitative observation of the variation in weld morphology as a function of material type and high-energy beam process. Consideration of the material properties and physical nature of the processes allows comparisons to be made which can help guide decisions regarding process selection and weld development. In application of any high energy beam process for specialty or critical applications, such as nuclear applications, precise control of all process variables is key. This mandates that material selection, forming, machining, cleaning, handling and joining must be precisely defined and controlled for each application.

Figure 19. Near full penetration laser weld in rhenium displaying large grain growth and reduced occurrence of porosity.

In comparing these two high energy beam processes, regarding their application to the joining of refractory metals for nuclear applications, one can first consider the differences between the beam generating systems. The high voltage systems typical of electron beam generators often employ oil immersion high voltage tanks. This can be a source of potentially radioactively contaminated mixed waste during oil change out. This is due to the relatively short high voltage cables lengths hindering the remote placement of the beam generator outside a radiological controlled area. In contrast, fiber optic laser beam delivery may allow greater flexibility in the remote placement of the beam power supply with respect to processing operations. It should be noted that glove box interfaces with fiber delivered laser beam are still being developed and are undergoing testing to prove robust functioning.

The electron optics of EB gun are often larger and more massive than laser optics and either fixed to the EB chamber or they may be articulated with robust positioning systems. The EB optics are adjustable using magnetic lenses to adjust the beam focal length, and beam placement. Rapid modulation of the magnetic beam positioning coil currents allows great flexibility in tailoring the energy distribution of the beam to vary the spatial and temporal character of the heat source to optimize weld shape and process stability. Electron filament emitters have a limited lifetime on the order of 100 hours. Replacement of filaments for nuclear applications may require the generation of mixed radiological waste and the potential for radiological exposure to personnel. Laser optics often provide a choice of fixed focal length lens but offer little flexibility at the cost of large focal spot sizes as a function of focal length. This is a significant detriment of the laser process verses the electron beam process, particularly when optimizing welding in a deep keyhole mode of melting to reduce spatter, voids and increase keyhole stability. The robustness and maintenance of laser optics in a radiologically controlled environment is yet to be fully determined by use in industrial applications.

The long focal length of the electron beam can allow placement of the beam into hard to reach joints provided there is a line of sight of the beam to the joint. Although charged particles of materials with high vapor points can travel back up the electron beam and cause arcing within the electron gun, this is often easily controlled by choice of longer focal lengths. Lasers with relatively shorter focal lengths can suffer from damaging back reflections that can cause heat and vapor damage to optical components. Tilting of the laser output optics can avoid back reflection problems but our preliminary observations indicate it may affect weld shape and stability in keyhole mode welding.

The physical constraints of the electron beam vacuum chamber place limitations of the size of parts that may be welded. Although large chamber machines have been produced and used effectively the associated vacuum technology used to pump down EB chambers is complex, time consuming, and requires regular maintenance. Again, when welding nuclear systems, there would be a potential of radiological contamination of vacuum oil and the creation of a mixed waste stream. High-energy electron beam welding can produce x-rays that further complicate protection of and access to the EB chamber. EB chambers can often feature water-cooled heat shields at the chamber ceiling to protect against the potentially large amounts of heat that can be generated by the process. In comparison, the introduction of lasers into glovebox can suffer from many of the same geometric limitations, although inert atmosphere purification systems can generally be smaller and less complex than EB vacuum systems. No pump down time would be required for laser welding unless it is performed in a vacuum. Laser welding could be performed in any mix of inert gases or a vacuum with the ability to these atmospheres into a container, ie: a nuclear fuel rod. The laser welding process

generates no x-rays. It is important to note when comparing the costs of laser verses EB systems for refractory metal welding one should consider the cost of custom designed, high purity inert glovebox and associated motion systems. These additional costs could amount to hundreds of thousands of dollars. One laser could provide multiple fiber output to a number of processing glovebox, although consideration regarding the shared laser resource, control and single point failure would need to be addressed.

The physics of electron and photon interactions with materials are beyond the scope of this report but practical considerations regarding beam absorption and beam-plume-plasma interactions cannot be ignored. Electron beams are more efficient in the deposition of energy into materials than are laser beams thus producing more melting per kilowatt. The electron beams produce vaporization and ionized species but beam delivery is generally not affected to a practical degree. The electron beam may however be affected by spurious magnetic fields, thus deflecting the beam off the weld joint. Lasers operating a high powers do not produce x-rays and do not have the requirement for lead shielding as do high voltage EB systems. They do however, require shielding of the optical radiation that can travel long distances and produce serious hazards if containment systems are not properly engineered. Plumes of gases, particulate and absorptive plasmas can form above laser welds and greatly affect process stability and weld morphology. In the course of evaluation of this system, large bright plumes formed above the welds but were not suppressed or blown away. Previous plume vs no plume, Ar vs He studies on stainless steel using this laser showed little effect on penetration although characterization of these effects would be warranted for process optimization for a specific application.

Microstructural evolution of laser verses EB welds will be similar under conditions of similar cooling rates. Differences in weld and defect morphology will occur as a result of focal spot sizes, energy absorption and keyhole dynamics. This is a topic for further study. A large body of weld performance data has been generated for the performance of electron beam welds in refractory metal systems. Of particular significance are data collected from long term testing of mechanical, creep and corrosion performance under reactor and high temperature irradiation testing. This data may have to be generated for laser welding before consideration for critical applications.

Summary and Conclusions

A state-of-the-art continuous wave diode pumped industrial laser welding system has demonstrated the capability to produce welds in a variety of refractory metals. The high beam quality of a fiber optically delivered Nd:YAG laser beam allows sufficient energy density at the focal spot to produce a keyhole mode of melting at high travel speeds and produce high aspect ratio welds without excessive grain growth in the fusion or heat affected regions of the weld. Furthermore, the fiber optic delivery facilitates introduction of the multi-kilowatt laser beam into a controlled atmosphere environmental chamber required to prevent contamination of the solidifying refractory metal weld pool with interstitial elements such as oxygen, nitrogen, or hydrogen. Side by side comparisons with electron beam welds demonstrate that despite larger focal spot sizes and a decreased laser energy absorption in comparison to EB welds, structural welds can be made in material thickness typical for many advanced materials applications. The disadvantages of fixed output optics, potential damage from laser energy back-reflections and short focal lengths should be balanced with distinct advantages. Advantages may include reduced process complexity, increased process flexibility thus allowing these lasers to be considered as a candidate process for joining refractory metals.

Acknowledgements

This research was funded under Department of Energy Contract No. W-7405-ENG-36. We also thank Dr. Patrick Hochandel of Los Alamos National Laboratory, Metallurgy Group for critical review of the paper.

References

1. J. R. Keeler, "The Selection of Cladding and Structural Materials", Reactor Handbook, Second Edition, Vol. 1 Materials, Edited by T. R. Tipton Jr., Interscience Publishers, Inc. New York, (1960), pages 477 – 481.
2. G. G. Lessman, "The Comparative Weldability of Refractory Metal Alloys", *Welding Journal*, 45, (12), Research Supplement, 540-s to 560-s, (1966).
3. J. Milewski, C. Hoth, "Welding Processes for Fuel Pin Fabrication", *6th Symposium on Space Nuclear Power Systems*, The Institute for Space Nuclear Power Studies, Albuquerque, New Mexico, January 9-12, 1989.
4. G. G. Lessman, R. E. Gold, "Determination of Weldability and Elevated Temperature Stability of Refractory Metal Alloys: II Long Term Stability of Refractory Metal Alloys", NASA CR-1608, (Westinghouse Astronuclear Lab., Pittsburgh, PA) National Aeronautics and Space Administration, Washington D.C., September 1970.
5. *Proceeding of Symposium on Refractory Alloy Technology For Space Nuclear Power Applications*, Oak Ridge National Laboratory, August 10-11, 1983, Edited by R. H. Cooper, Jr., E. E. Hoffman, Office of Scientific Information, USDOE, CONF-8308130, January 1984.
6. F. Smith, J. Milewski, " Electron Beam Welding Comes Through In An Exacting Job", *Welding Journal*, Vol. 80, No. 6, June 2001, pp. 43-46.
7. D. L. Olson, B. Mishra, D. W. Wenman, " Welding, Brazing and joining of refractory metals and alloys.", *Mineral Processing and Extractive Metallurgy Review*, 2001, v.22, no. 1-3 SPEC. ISS, p1-23.
8. J. Bliedtner, T. Heyse, D. Jahn, G. Michel, H. Müller, D. Wolff, "Advances in Diode Lasers Increase Weld Penetration", *Welding Journal*, Vol. 80, No. 6, June 2001, pp. 47-51.